International Journal of Nanomedicine

Dovepress
open access to scientific and medical research

Open Access Full Text Article

ORIGINAL RESEARCH

Combined Therapy of Experimental Autoimmune Uveitis by a Dual-Drug Nanocomposite Formulation with Berberine and Dexamethasone

Chang Huang[1,2,*], Zhutian Zhang[1,2,*], Jifeng Gu[3,*], Dan Li[1,2], Shunxiang Gao[1,2], Rong Zhang[1,2], Rong Shi[4], Jianguo Sun[1,2]

[1]Eye Institute and Department of Ophthalmology, Eye & ENT Hospital, Shanghai Medical College, Fudan University, Shanghai, 200031, People's Republic of China; [2]NHC Key Laboratory of Myopia, Shanghai Key Laboratory of Visual Impairment and Restoration, Fudan University, Shanghai, 200031, People's Republic of China; [3]Department of Pharmacy, Eye & ENT Hospital, Shanghai Key Laboratory of Bioactive Small Molecules, Fudan University, Shanghai, 200031, People's Republic of China; [4]Science and Technology Experimental Center, Shanghai University of Traditional Chinese Medicine, Shanghai, 201203, People's Republic of China

*These authors contributed equally to this work

Correspondence: Jianguo Sun, Eye Institute and Department of Ophthalmology, Eye & ENT Hospital, Fudan University, Shanghai, 200031, People's Republic of China, Email jgsun@fudan.edu.cn; Rong Shi, Science and Technology Experimental Center, Shanghai University of Traditional Chinese Medicine, Shanghai, 201203, People's Republic of China, Email rongshi56@126.com

Purpose: Autoimmune uveitis is a kind of sight-threatening ocular and systemic disorders. Recent treatments on autoimmune uveitis still remain many limitations due to extreme complexity and undetermined pathogenesis. In this study, a novel dual-drug nanocomposite formulation is developed to treat experimental autoimmune uveitis by a combined and sustained therapy method.

Methods: The dual-drug nanocomposite formulation is constructed by integrating berberine (BBR)-loaded mesoporous silica nanoparticles (MSNs) into dexamethasone (DEX)-loaded thermogel (BBR@MSN-DEX@Gel). The BBR@MSN-DEX@Gel is characterized by transmission electron microscopy, dynamic light scattering, Fourier transform infrared spectrometer and rheometer. The in vitro drug release profile, cytotoxicity and anti-inflammation effectiveness of BBR@MSN-DEX@Gel on lipopolysaccharide-stimulated human conjunctival epithelial cells are investigated. After the in vivo drug release profile and biosafety of the dual-drug nanocomposite formulation are confirmed, its treatment effectiveness is fully assessed based on the induced experimental autoimmune uveitis (EAU) Lewis rat's model.

Results: The dual-drug nanocomposite formulation has good injectability and thermosensitivity, suitable for administration by an intravitreal injection. The BBR@MSN-DEX@Gel has been found to sustainably release both drugs for up to 4 weeks. The carrier materials have minimal in vitro cytotoxicity and high in vivo biosafety. BBR@MSN-DEX@Gel presents obviously anti-inflammatory effectiveness in vitro. After administration of BBR@MSN-DEX@Gel into Lewis rat's eye with EAU by an intravitreal injection, the nanocomposite formulation significantly suppresses inflammatory reaction of autoimmune uveitis via a dual-drug combined and sustained therapy method, compared with the equivalent dose of single-component formulations.

Conclusion: BBR@MSN-DEX@Gel serves as a promising dual-drug nanocomposite formulation for future treatment of autoimmune uveitis.

Keywords: nanocomposite formulation, combined and sustained therapy, dexamethasone, berberine, experimental autoimmune uveitis

Introduction

Uveitis, described as the intraocular inflammation of uveal tract (eg, iris, ciliary body, and choroid, etc.), is one of the leading causes of visual impairment among the working-age population.[1] Generally, it can be classified into infectious and non-infectious uveitis, and noninfectious uveitis is related to systemic or idiopathic autoimmune conditions, known as autoimmune uveitis.[2] The estimated prevalence of autoimmune uveitis is 121/100,000 in the United States.[3] Glucocorticoids (eg, dexamethasone (DEX)) remain the primary therapy for autoimmune uveitis for their powerful anti-inflammatory activities.[4] However, long-term DEX treatments may cause serious ocular or systemic adverse effects.[5] As is well known, autoimmune

Received: 3 May 2023
Accepted: 24 July 2023
Published: 31 July 2023

uveitis is a very complicated disease associated with dozens of etiologies and multifactorial pathological mechanisms.[1] Thus, alternative strategies, such as combined therapy targeting different pathophysiological mechanisms, should be explored to treat autoimmune uveitis. Berberine (BBR), a type of isoquinoline alkaloids, is known for its anti-inflammatory,[6] anti-microbial[7] and anti-diabetic[8] properties, with excellent therapeutic effects especially in autoimmune uveitis.[6] In this study, BBR and DEX were chosen as therapeutic agents to develop a combination therapy strategy for autoimmune uveitis.

Topical DEX instillation turns out to be a powerful treatment for ocular anterior segment diseases, but it is not effective for treating ocular posterior segment diseases, mainly owing to poor drug permeability through ocular physiological barriers.[9] Alternatively, drug administration by intravitreal injection has been validated as a realistic method for treatments of ocular posterior segment diseases.[10] However, intravitreal administration of small molecule drugs, such as DEX (MW 434.5) or BBR (MW 371.8), tends to provide only a short-time treatment effect, mainly due to rapidly consumption and metabolism through the aqueous humor circulation.[11,12] Thereby, it is necessary to construct new formulations with dual-drug loading and sustained releases of DEX and BBR to improve drug bioavailability and prolong the duration of drug action for subsequently improving treatment efficacy upon autoimmune uveitis.

More recently, ocular drug delivery systems (DDSs) have become common approaches to enhance drug bioavailability and prolong duration time.[9,13] The application of nanomaterials in the DDSs has been rapidly developed in recent years because of their advantages, such as targeting,[14] artificially modifiable,[15] reduced drug toxicity[16] and improved drug bioavailability.[17] There have also been various reports on DEX DDSs for ophthalmic disorders based on hydrogels,[18,19] micelles,[20] dendrimers,[21] cubosomes,[22] microcrystals,[23] and lipid nanoparticles,[24,25] especially the commercially available Ozurdex® implant (comprising poly(lactic-co-glycolic acid) (PLGA) carrier material and DEX), for the treatment of diabetic macular edema[26,27] and autoimmune uveitis via an intravitreal administration.[28] Similarly, several DDSs have also been developed for BBR delivery,[29] such as dendrimer-liposome compound[30] and gelucires.[31] However, no available DDS has been developed to co-deliver DEX and BBR for treatment of autoimmune uveitis.

In this study, we expected to construct an injectable platform based on mesoporous silica nanoparticles (MSNs)/thermo-sensitive nanogel (thermogel) to simultaneously deliver DEX and BBR to improve long-term therapeutic efficacy on auto-immune uveitis. MSNs have been widely used in the development of DDSs[32–35] owing to the high pore volume, well-defined pore structure, large specific surface area, and tunable pore size, especially biocompatibility and biodegradability.[36,37] Moreover, thermogel has also been applied in the biomedical fields, especially in DDSs.[38–40] The thermogel precursor solution presents a free-flowing sol-phase below room temperature, while it may spontaneously convert into gel-phase when the temperature rises to physiological temperature.[41,42] In this course, targeted drugs can be easily loaded into the polymer micelles when the amphiphilic triblock copolymers of PLGA–PEG–PLGA dissolve in an aqueous solution and spontaneously undergo molecular chain self-assembly.

Herein, a dual-drug nanocomposite formulation was prepared by embedding BBR@MSN into thermogel loaded with DEX (BBR@MSN-DEX@Gel), as shown in Scheme 1. The physical properties, in vitro drug releases, cytotoxicity, and anti-inflammation effect of BBR@MSN-DEX@Gel were investigated. Furthermore, the treatment effectiveness of the dual-drug nanocomposite formulation was fully assessed based on the experimental autoimmune uveitis (EAU) Lewis rat's model.

Materials and Methods

Materials

Berberine (BBR) was bought from MedChemExpress (Shanghai, China). Dexamethasone acetate (DEX), lipopolysaccharide (LPS), tartaric acid (TA), N-hydroxy succinimide (NHS), 1-(3-dimethylaminopropyl)-3-ethylcarbodiimide hydrochloride (EDC) and Dulbecco's Modified Eagle Media (DMEM) were all obtained from Sigma-Aldrich (Shanghai, China). PriMed-iCELL-001 was purchased from Ruian BioTechnologies (Shanghai, China). Fetal bovine serum (FBS) and phosphate buffered saline (PBS) were bought from Thermo Fisher (Shanghai, China). MSNs were bought from XFNANO (Nanjing, China). IRBP peptide R16 (1177–1191, ADGSSWEGVGVVPDV, 98% purity) and complete freund's adjuvant (CFA) were synthesized by Sangon (Shanghai, China). Mycobacterium tuberculosis H37RA (TB) was bought from Difco Laboratories (Detroit, USA). The copolymer of $PLGA_{1604}$–PEG_{1500}–$PLGA_{1604}$ was bought from Tanshtech Co., Ltd (Guangzhou, China). Propidium iodide (PI) and calcein acetoxymethyl ester (Calcein-AM) were bought from Servicebio (Wuhan, China).

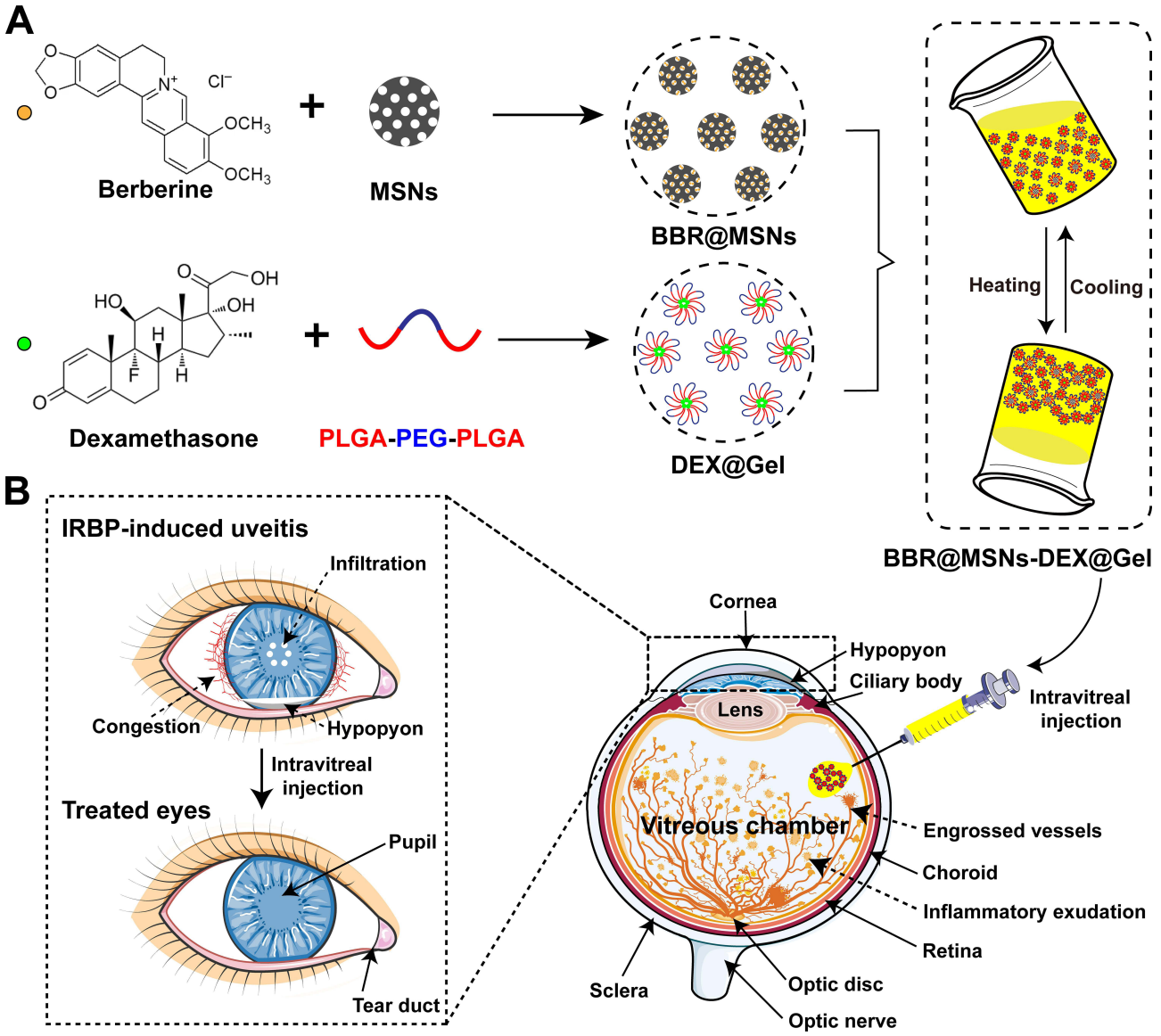

Scheme 1 Schematic representations of preparation procedure (**A**) and intravitreal administration (**B**) of the dual-drug nanocomposite formulation with berberine and dexamethasone (BBR@MSN-DEX@Gel) for sustained and combined therapy on experimental autoimmune uveitis (EAU) induced by IRBP peptide.

Tetracaine eye drops were purchased from Santen (Osaka, Japan). Cell Counting Kit-8 (CCK-8) assay was obtained from Dojindo Molecular (Shanghai, China). Dichloromethane and anhydrous ethanol were bought from Lingfeng Chemical Reagents Co., Ltd (Shanghai, China).

Preparation of BBR@MSN-DEX@Gel

The surface modification process of MSNs for improving drug loading was illustrated as follows. At first, TA (100.0 mg), EDC (383.1 mg) and NHS (383.4 mg) were all dissolved in ethanol aqueous solution (30 mL, 50%). Then MSNs (100.0 mg) were added, and the solution was further stirred for 3 h (300 rpm, 37 °C). Subsequently, the modified-MSNs were obtained by centrifugation (12,000 rpm, 3 min) and dried naturally. BBR (50.0 mg) was dissolved in dichloromethane (10.0 mL), and the surface-modified MSNs were added into the BBR dichloromethane solution. The solvent was then evaporated naturally with continuous stirring (300 rpm), and the BBR@MSN dry powder was obtained eventually.

After that, 3.0 g of PLGA–PEG–PLGA copolymer was added into distilled water (9.0 mL) and the solution was continuously stirred for 3 d (600 rpm, 4 °C) to form thermogel precursor solution (25% w/w). After 8.0 mg of DEX was

added, the thermogel solution (4.0 g) was stirred for another 3 h (600 rpm, 4 °C). BBR@MSN (40.0 mg) was then added to the above thermogel precursor solution to prepare BBR@MSN-DEX@Gel. BBR@MSN-DEX@Gel thermogel precursor solution (1.0 μL) contains 2.0 μg DEX, 3.3 μg BBR, 6.7 μg MSNs and 0.25 mg copolymer. All MSNs and BBR@MSN samples were sterilized by Ultraviolet (254 nm, 30 min). All thermogel precursor samples were sterilized with a filter membrane (0.22 μm, 4 °C).

Characterizations of BBR@MSN-DEX@Gel

Initially, the particle size and morphology of MSNs were observed by transmission electron microscope (TEM, Tecnai G2F20S-TWIN, USA). Nitrogen adsorption-desorption isotherms were obtained by a small TriStar 3000 analyzer (77 K, USA). Fourier transform infrared spectroscopy (FTIR) spectra were acquired at a resolution of 500–4000 cm^{-1} by the Nicolet 6700 FTIR spectrometer (Thermo Fisher, USA). The specific surface area, pore volume and pore size distribution were calculated by the Brunauer–Emmett–Teller (BET) and the Barrett–Joyner–Halenda (BJH) methods. Besides, the zeta potential of MSNs in distilled water was measured by the Zetasizer (Malvern Instruments, Malvern, UK). The sol–gel transition of thermogel precursor solution was investigated by detecting the rheological property of the copolymer (PLGA–PEG–PLGA) aqueous solution (25% w/w) with/without BBR and MSN-DEX. The rheological property was measured by a rheometer (Malvern, USA) with a 60-mm diameter parallel plate, a 0.5 °C/min heating rate and a 10 rad/s oscillatory frequency. The storage modulus *G*' and loss modulus *G*" were determined in the temperature range of 15–55 °C.

In vitro Drug Release

The in vitro drug releases from BBR@MSN, DEX@Gel and BBR@MSN-DEX@Gel were investigated as follows. At first, BBR@MSN (0.66 mg BBR), DEX@Gel (0.2 g, 2.0 mg/mL of DEX) or BBR@MSN-DEX@Gel (0.2 g, 2.0 mg/mL of DEX and 3.3 mg/mL of BBR) was added into a dialysis bag (cut-off *M*w: 50 kDa). The dialysis bag with samples was put in a vial (100 mL), which was then incubated in a water bath with a temperature of 37 °C for 30 min. After hydrogel formation in the DEX@Gel and BBR@MSN-DEX@Gel groups, 50 mL of warm PBS (37 °C, pH 7.4) containing 0.025% (w/w) NaN_3 was added in the vial as the release medium (n = 4). The vials with samples were shaken at 50 rpm and 37 °C in a shaker (DKZ-3B, Shanghai Yiheng). Later, at the time point of 0, 1, 4, 7 h and 1, 2, 4, 7, 14, 21, 35, 42 d, 2 mL of leaching solution was withdrawn and then another 2 mL of fresh PBS was refilled afterwards. The withdrawn aliquot samples were rapidly stored under −20 °C till measurements. The concentrations of BBR and DEX were determined by UV-Vis's absorbance at the detection wavelengths of 346 and 240 nm (NanoDrop 2000, Thermo Scientific, Waltham, MA). The average results were calculated from 4 parallel samples (n = 4).

In vitro Cytotoxicity

The human conjunctival epithelial cells (HConEpics) and mice corneal epithelial cells (MIC-iCELL-m001) were used to investigate the in vitro cytotoxicity of MSNs solution (6.7 μg/μL), thermogel precursor solution (25% w/w), BBR solution (3.3 μg/μL), BBR@MSN solution (3.3 μg/μL BBR), DEX solution (2.0 μg/μL), DEX@Gel precursor solution (2.0 μg/μL DEX) or BBR@MSN-DEX@Gel precursor solution (3.3 μg/μL BBR and 2.0 μg/μL DEX). HConEpics were obtained from the American Type Culture Collection (ATCC, USA), and MIC-iCELL-m001 was obtained from Ruian BioTechnologies (Shanghai, China). MIC-iCELL-m001 was cultured in PriMed-iCELL-001 medium, whereas HConEpics in 10% DMEM, with 1.0×10^4 cells/96-well. After 4 μL of components of different formulations were, respectively, added into the culture medium (0.1 mL, n = 12), the cells were then incubated for another 24 h. The Calcein-AM/PI staining was used to identify live and dead cells.[43] And a fluorescence microscopy (Leica, Germany) was used to observe live and dead cells. Furthermore, cell viability was detected by CCK-8 assay (n = 6) as previously reported.[44] A micro plate reader (Synergy H1 Hybrid Reader, VT) was used to detect the UV absorbance of each 96-well at 450 nm. The blank culture medium was used as the control. The result of in vitro cytotoxicity was expressed as the relative percentage of cell viability compared to the control group (100%).

In vitro Anti-Inflammatory Effectiveness

HConEpics were cultured overnight (37 °C, 5% CO_2) in 96-well plates (1.0×10^4 cells/well). Then, 4 μL of thermogel precursor solution (25% w/w), MSN solution (6.7 μg/μL), BBR solution (3.3 μg/μL), BBR@MSN solution (3.3 μg/μL), DEX solution (2.0 μg/μL), DEX@Gel precursor solution (2.0 μg/μL) or BBR@MSN-DEX@Gel precursor solution (3.3 μg/μL BBR and 2.0 μg/μL DEX) was added to each well (n = 8). After being co-incubated for 2 h, HConEpics were stimulated with lipopolysaccharide (LPS) (0.125 μg/μL, 2 μL) for another 24 h. Then, the supernatant in each well was collected, and the concentration of interleukin-17A (IL-17A) was measured by Human IL-17A ELISA kit (Thermo Fisher, USA). The cells without any operations were set as the control. All experiments were performed in triplicate (mean ± SD, n = 4).

Animal Experiment

The ethical and legal approval with No. of PZSHUTCM2306220010 was obtained from Shanghai University of Traditional Chinese Medicine prior to the commencement of the study. All animal experiments were carried out in accordance with the Association for Research in Vision and Ophthalmology Statement for the Use of Animals in Ophthalmic and Vision Research and the guidelines of the Animal Care and Use Committee of Eye and ENT Hospital of Fudan University and Shanghai University of Traditional Chinese Medicine. Male Lewis rats (4–6 w, 240–260 g) were obtained from Shanghai Sippr-BK (Shanghai, China) and housed under a pathogen-free condition with alternating 12/12 h light–dark cycle with free access to standard normal diet and water. Lewis rats were anesthetized by intraperitoneal injection of 0.5% sodium pentobarbital, followed by topical anesthesia with tetracaine eye drops for administration and observation. Healthy Lewis rats (n = 70) were randomly divided into 7 groups: normal control group (NC, n = 5 rats with 10 eyes), IRBP-induced EAU (left eyes, n = 65 eyes), IRBP-induced EAU with 5 different treatments (right eyes, n = 13 eyes), including BBR, BBR@MSN, DEX, DEX@Gel and BBR@MSN-DEX@Gel.

Induction of EAU Model and Treatment Formulations

A subcutaneous injection of 300 μL IRBP peptide R16 (540 μg/mL) and TB (100 μg) emulsified in CFA was performed on each Lewis rat in all IRBP-induced EAU groups (total of 65 rats), while a subcutaneous injection of only 300 μL TB (100 μg) emulsified in CFA was operated to the NC group (5 rats). Further, the IRBP-induced EAU rats were randomly assigned to 5 treated groups, and all left eyes without any treatments (untreated group). In the treated groups, IRBP-induced EAU eyes (n = 13 eyes) were treated with an intravitreal injection (4 μL) of BBR solution (3.3 μg/μL), BBR@MSN (3.3 μg/μL BBR), DEX solution (2.0 μg/μL), DEX@Gel (2.0 μg/μL DEX), or BBR@MSN-DEX@Gel (3.3 μg/μL BBR, 2.0 μg/μL DEX). More specifically, the intravitreal injection was performed by inserting a microvolume syringe (0.26 mm, Bolivian Dove, Shanghai, China) into the vitreous at a site of 1 mm posterior to the limbus of rat eyes.

Evaluation of Inflammation Reaction

After EAU induction, the observation time points were set at 1, 2 and 4 w according to the previous report.[45] The inflammation reaction of Lewis rats' eyes in each group was observed and the images were taken with a Canon EOS 850D (Shanghai, China). Furthermore, the severity level of inflammation reaction was scored according to the reported criteria,[46] as follows: no inflammation (0), iris congestion and mild retinal vasculitis (1), mild fibrous tissue exudation in anterior chamber (2), moderate exudation and mild empyema in anterior chamber (3), and severe bleeding and empyema in anterior chamber (4).

In vivo Drug Release from BBR@MSN-DEX@Gel

Accompanied by the evaluation of the treatment effectiveness of BBR@MSN-DEX@Gel on IRBP-induced EAU, the in vivo drug release was also investigated. At week 2 after administration, four Lewis rats in each group were randomly selected and sacrificed, and the eyeballs (n = 4) were enucleated. The cornea, vitreous body, and retina were carefully isolated from the eyeballs. The concentrations of BBR and DEX in the tissue samples in each group were measured by high-performance liquid chromatography-tandem mass spectrometry (HPLC-MS/MS), according to the previous methods.[44]

Histopathological Examination

At different time points (1, 2 and 4 w), three Lewis rats were sacrificed in each group and the eyeballs (n = 3) were enucleated for histopathological examination. The eyeballs were fixed and embedded in paraffin. Then, the retinal tissue sections (3 μm) were obtained and stained with hematoxylin & eosin (H&E) and Masson. The pathohistological score standard was referred to the *Caspi's* scores.[47] That is, 0: no retinal inflammation, normal structure; 0.5: mild inflammatory cell infiltration in the retina or vitreous, with/without damages to photoreceptors; 1: mild inflammatory cell infiltration and/or damages to the outer segment of the photoreceptor in the retina; 2: mild to moderate inflammatory cell infiltration and/or damages of the retina extending to the outer nuclear layer; 3: moderate to significant inflammatory cell infiltration and/or damages of retina involving internal limiting membrane; 4: severe inflammatory cell infiltration and/or whole-layer destruction of the retina.

Statistical Analysis

Data were expressed as mean ± SD. The significant difference was determined by two-way ANOVA. Difference $p < 0.05$ is considered statistically significant. Each experiment was conducted in triplicate independently. All analyses were performed using SPSS (SPSS Inc., USA).

Results

Characterizations of BBR@MSN-DEX@Gel

MSNs were discrete spheres with an average diameter of 33.5 ± 5.2 nm and a pore size of 2.8 nm (Figure 1A and B). The N_2-adsorption-desorption curves of MSNs are shown in Figure 1B. BET measurements were lighted on the pore features of MSNs with 564.7 m^2/g surface area and 1.6 cm^3/g pore volume. Moreover, the hydrodynamic diameter and zeta potential of MSNs were 91.3 nm and −25.2 mV, respectively (Supplement Information, Figure S1). Figure 1C depicts the FTIR spectra of BBR, MSNs and BBR@MSNs. In the MSN spectrum, the characteristic bands included 798 cm^{-1} (assigned to the ν(SiOSi)) and 1050–1200 cm^{-1} (peaked at 1085 cm^{-1}, corresponding to the δ(SiOSi)).[32] Also, in the spectrum of BBR, the three characteristic absorption bands were detected at 1590 cm^{-1} (ν(C=C)), 1300 cm^{-1} (ν(C-O)), and 1060 cm^{-1} (ν(C-H)).[48] Furthermore, the above characteristic bands of BBR and MSNs were simultaneously found in the spectrum of BBR@MSN, which confirmed the successful loading of BBR into MSNs.

The BBR@MSN-DEX@Gel was prepared by dispersing BBR@MSN into the thermogel precursor solution with DEX. The results of rheological properties of the thermogel precursor solution with or without BBR@MSN and DEX are shown in Figure 1D. At 20 °C, the elastic modulus (G') of the thermogel precursor solution was lower than the viscous modulus (G''), which indicated that the thermogel precursor solution had a free-flowing sol state and good injectability. When temperature elevated, both G' and G'' increased simultaneously, which showed a poor free-flowing capacity. When G' and G'' were equal, the temperature site (close to 40 °C) was thought as the sol–gel transition temperature. In the gel-state, G' was more than G'', and both G' and G'' reached their peak values (638.8 and 478.4 Pa, respectively) near 46–48 °C. This sol–gel transition feature of the thermogel precursor solution is beneficial for its in vivo biomedical application, especially administration by an injection route. After being loaded with BBR@MSN and DEX, the BBR@MSN-DEX@Gel precursor solution presented similar rheological curves to those without drug-loading. Thus, the addition of BBR@MSN and DEX did not obviously affect the rheological properties of the thermogel precursor solution. As a consequence, BBR@MSN-DEX@Gel was suitable to be administrated by intravitreal injection.

In vitro Drug Release

The in vitro drug release from BBR@MSN, DEX@Gel or BBR@MSN-DEX@Gel was investigated (Figure 2). Generally, three phases, initial burst release (I), sustained release (II), and slow release (III), were observed during all 42 d (Figure 2A). In the first phase (I), the immediate BBR concentrations in the BBR@MSN and BBR@MSN-DEX@Gel increased sharply from 0 to 15.9 and 16.2 μg/mL on day 1 (Figure 2A), responding to ~21.9% and ~27.4% cumulative release, respectively (Figure 2B). This phenomenon was mainly attributed to the initial burst release. In

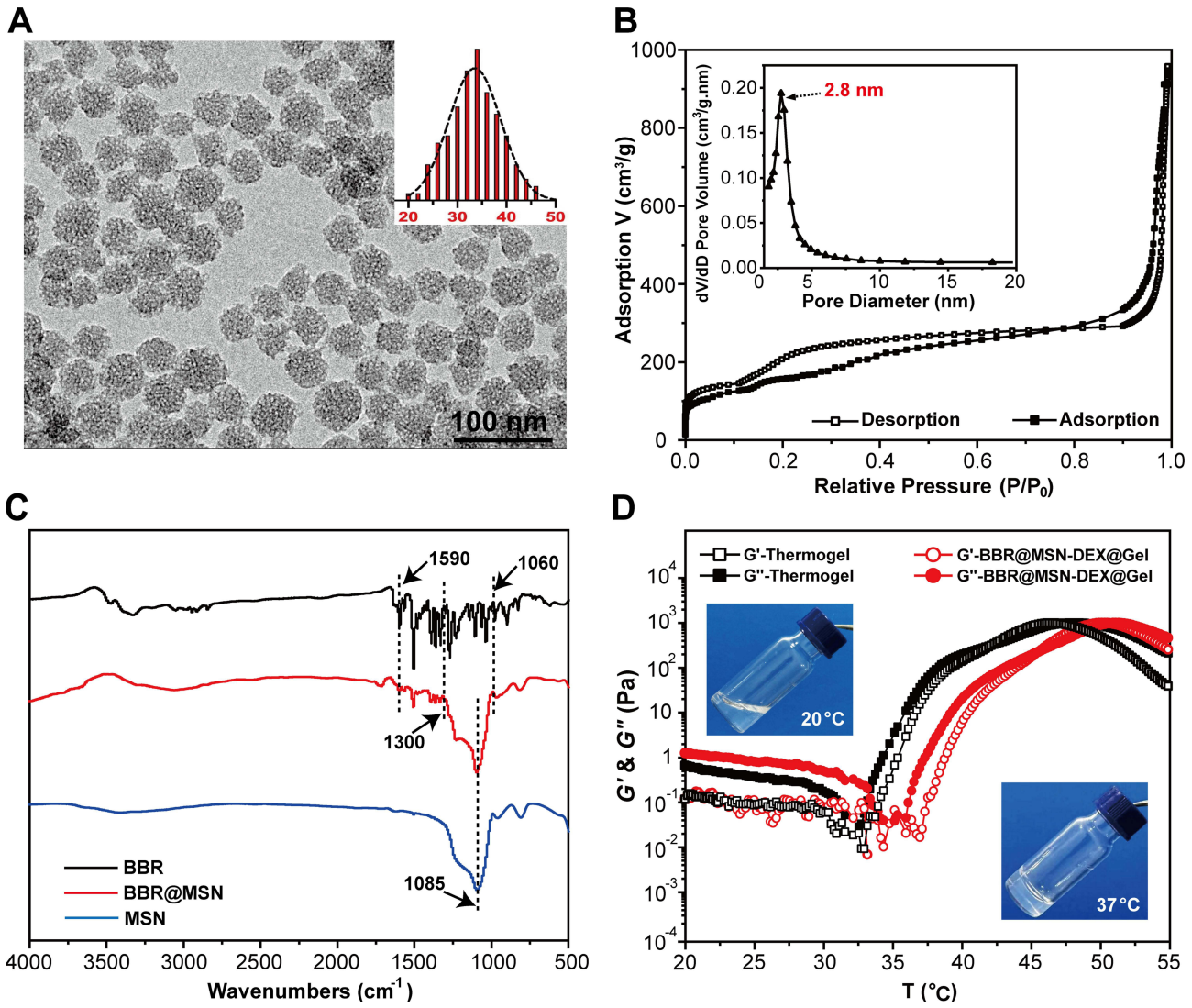

Figure 1 Characteristics of BBR@MSN-DEX@Gel. (**A**) Particle size and surface morphology of MSNs measured by transmission electron microscopy (TEM). (**B**) N_2 adsorption–desorption curves and the pore size distribution curve (the inserted image) of MSNs. The specific surface area, pore volume and pore size distribution were calculated by Brunauer-Emmett-Teller (BET) and Barrett-Joyner-Halenda (BJH) methods. (**C**) Fourier transform infrared spectroscopy (FTIR) spectra of BBR, BBR@MSN and MSNs. (**D**) Elastic modulus (*G'*) and viscous modulus (*G''*) of thermogel precursor solution with or without BBR@MSN and DEX; heating rates: 0.5 °C/min, oscillatory frequency: 10 rad/s. Moreover, the inserted image showed that BBR@MSN-DEX@Gel presented a sol-state at 20 °C and gel-state at 37 °C. All results were expressed as mean ± SD (n = 4).

the second phase (II), the immediate BBR concentration in BBR@MSN maintained a fluctuation state at a relatively high level (4.6–17.4 μg/mL), and the cumulative BBR release increased gradually to ~69.2% on day 28. However, BBR@MSN-DEX@Gel presented a lower immediate BBR concentration (3.3–6.8 μg/mL) and cumulative release (~48.7%) than BBR@MSN at the same period, which was probably owing to the more release obstruction and diffusion resistance caused by the carrier materials (MSNs and thermogel). During the last phase (III), the BBR release rate in both BBR@MSN and BBR@MSN-DEX@Gel slowed down, and the cumulative release curves ultimately reached a plateau up to 42 d.

The release profiles of DEX from both DEX@Gel and BBR@MSN-DEX@Gel were also investigated (Figure 2C and D). A similar three-phase release pattern of DEX was also observed in the DEX@Gel and BBR@MSN-DEX@Gel. Both of them experienced a burst release within 4 h, and the immediate DEX concentration reached 13.9 μg/mL in DEX@Gel and 24.7 μg/mL in BBR@MSN-DEX@Gel, responding to the cumulative release of 11.7% and 18.9%, respectively. Then the immediate DEX concentration in DEX@Gel maintained a fluctuation state at a relatively lower level (7.0–13.9 μg/mL), and the

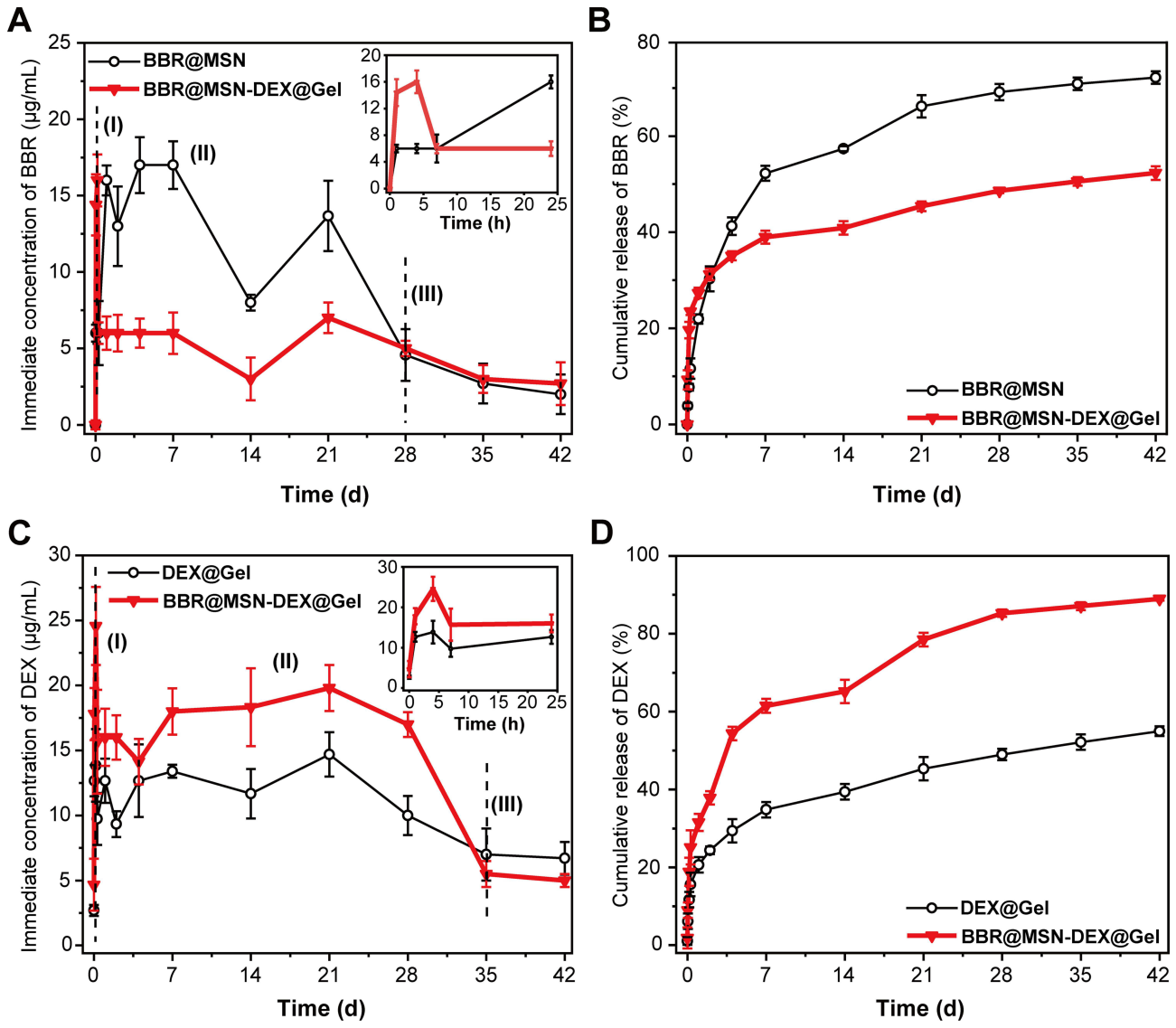

Figure 2 In vitro releases of BBR (**A** and **B**) and DEX (**C** and **D**) from BBR@MSN, DEX@Gel or BBR@MSN-DEX@Gel in PBS (pH = 7.4) at 37 °C. (**A** and **C**) present the immediate concentrations of BBR and DEX, while (**B** and **D**) show the cumulative drug releases. Results are shown as mean ± SD (n = 4).

cumulative DEX release increased gradually to 52.2% on day 35. BBR@MSN-DEX@Gel presented a higher immediate DEX concentration (5.5–24.7 μg/mL) and more cumulative release (~87.5%) than DEX@Gel at the same period (Figure 2D). This phenomenon was mainly due to the addition of BBR@MSN into the thermogel precursor solution with DEX, which broke the dynamic equilibrium of the thermogel precursor solution and made the polymer micelles partially disassembled and DEX released. The in vitro release pattern of BBR@MSN-DEX@Gel was helpful to maintain a long-term and sustained drug concentration for the anti-inflammatory treatment on EAU.

Cytotoxicity and Anti-Inflammatory Effectiveness

The in vitro cytotoxicity of MSN, thermogel, BBR, BBR@MSN, DEX, DEX@Gel and BBR@MSN-DEX@Gel was carefully evaluated by co-culturing them with HconEpics or MIC-iCELL-m001 and detecting the relative cell viability. Figure 3A shows the representative photos of HconEpics stained by Calcein-AM/PI for labeling live and dead cells. There was no obvious morphology and density difference of HconEpics among 7 groups. This result was further confirmed by the relative cell viability of HconEpics (Figure 3B) treated with MSN (100.7 ± 0.8%), thermogel (101.3 ± 1.0%), BBR (99.5 ± 2.9%), BBR@MSN (97.8 ± 4.3%), DEX (98.3 ± 2.1%), DEX@Gel (100.2 ± 3.3%) and BBR@MSN-DEX@Gel (100.8 ± 0.8%), compared with that in the

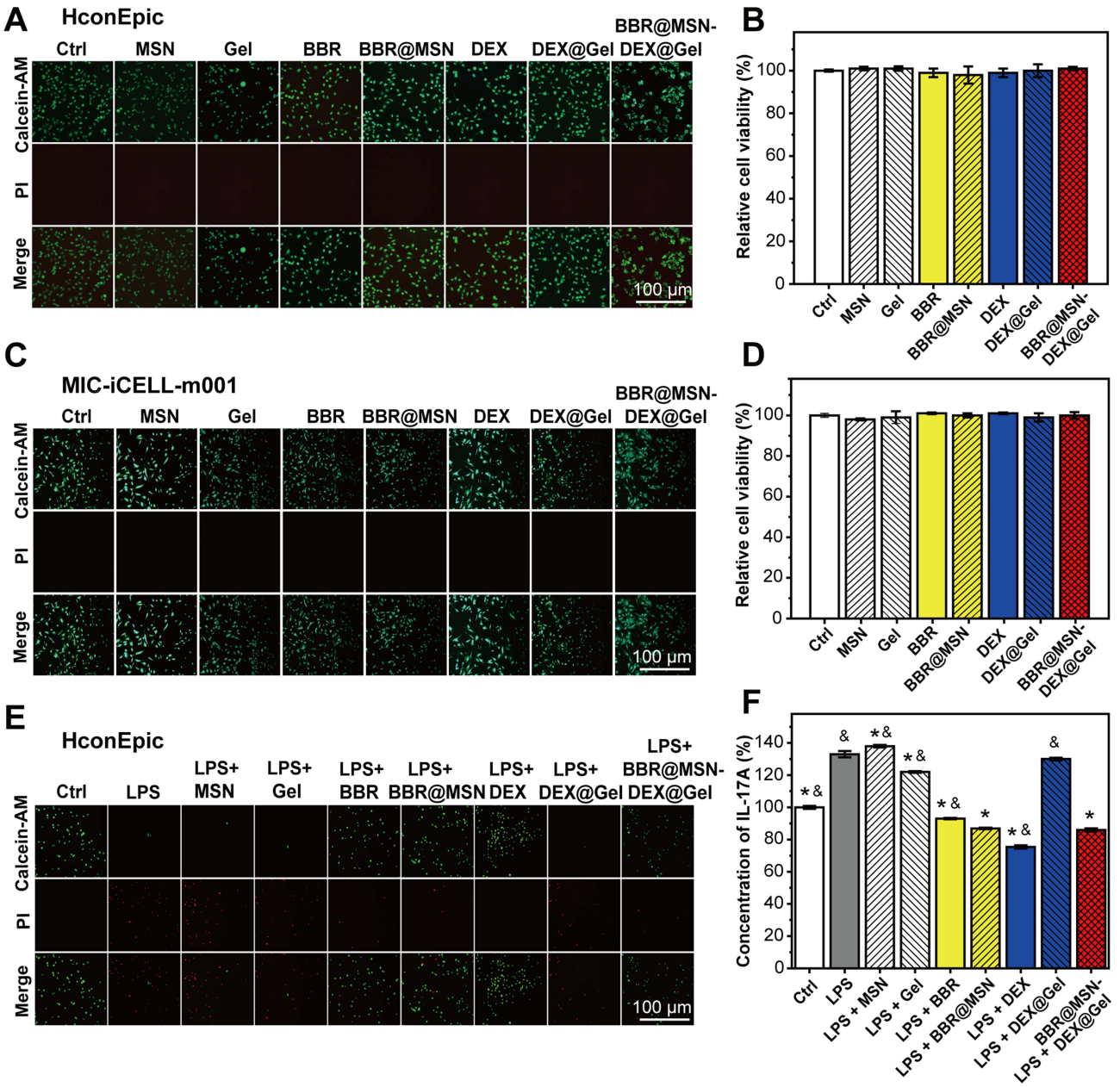

Figure 3 In vitro cytotoxicity of carrier materials (MSN and Gel) and different formulations, including BBR solution (BBR), BBR@MSN, DEX solution (DEX), DEX@Gel and BBR@MSN-DEX@Gel, and their anti-inflammatory effectiveness. (**A**) Representative photos and (**B**) relative cell viability of human conjunctival epithelial cells (HconEpics) (n = 6). (**C**) Representative photos and (**D**) relative cell viability of MIC-iCELL-m001 (n = 6). (**E**) Representative photos and (**F**) relative IL-17A concentration of LPS-stimulated HconEpics (n = 4). Cells without any manipulation were set as the control group (Ctrl, 100%). *p<0.05 vs LPS and $^{\&}p$<0.05 vs BBR@MSN-DEX@Gel (Two-way ANOVA).

control (100%). No significant difference was observed between all treated groups and the control group. Moreover, the above results were also supported by the cell photographs and cell viability of MIC-iCELL-m001, shown in Figure 3C and D. These results suggested that the carrier materials and therapeutic nanocomposite formulations had negligible cytotoxicity to both HconEpics and MIC-iCELL-m001. Thus, these nanoformulations could be applied for subsequent in vivo experiments.

Furthermore, the in vitro anti-inflammatory effects of the therapeutic nanocomposite formulations were also investigated based on the LPS-stimulated HconEpic model, and the inflammatory reaction was evaluated by an IL-17A assay, which was the principal mediator in autoimmune disorders.[49] As shown in Figure 3E, LPS-stimulation caused more dead cells, and the follow-up treatments by different formulations might rescue the cell death, especially BBR solution,

BBR@MSN, DEX solution, and BBR@MSN-DEX@Gel. The above treatment effectiveness was also confirmed by detecting IL-17A levels in all 7 groups. When the IL-17A level in the control group (without any manipulation) was set as 100%, LPS-stimulation caused a significantly elevated IL-17A level (132.7 ± 1.9%), indicating a more severe inflammatory reaction (Figure 3F). The treatment only with MSN or thermogel showed no therapeutic effectiveness (137.5 ± 0.8% and 121.7 ± 0.5%). However, all therapeutic formulations inhibited inflammatory reactions induced by LPS and presented a decreased IL-17A level. Compared to the LPS-stimulated group (132.7 ± 1.9%), the DEX group showed the strongest anti-inflammation effect and the lowest IL-17A level (75.5 ± 1.0%, $p<0.01$), followed by BBR@MSN-DEX@Gel (85.7 ± 0.9%), BBR@MSN (86.9 ± 0.5%, $p<0.05$) and BBR group (93.0 ± 0.4%). The poorest anti-inflammatory effect was observed in the DEX@Gel group (129.7 ± 0.8%), which might result from the less short-term DEX release (~20.6% within the first 24 h). Obviously, the BBR@MSN-DEX@Gel indicated a lower IL-17A level (85.7 ± 0.9%) and better anti-inflammatory effectiveness than DEX@Gel, which was mainly due to the more DEX release (~31.5% within the first 24 h in Figure 2D) and the adjuvant therapy provided by the simultaneously released BBR from BBR@MSN-DEX@Gel (~27.4% within the first 24 h). It should be noted that although there was no significant difference in IL-17A level between BBR@MSN and BBR@MSN-DEX@Gel, the anti-inflammatory effect of DEX in the BBR@MSN-DEX@Gel group did exist due to its lower BBR release (Figure 2A and B). These results successfully confirmed the in vitro treatment efficacy of BBR@MSN-DEX@Gel on LPS-stimulated inflammatory reaction.

In vivo Treatment Effectiveness of BBR@MSN-DEX@Gel

After administration of therapeutic formulations in IRBP-induced EAU eyes, the manifestations of the iris and anterior chamber in EAU and all treated eyes were observed. All taken photographs were scored in terms of abnormal pupil contraction, engrossed blood vessels or hypopyon according to the set criteria (Figure 4A). The representative photographs of the anterior segment in EAU and all treated eyes are shown in Figure 4B. IRBP-induced EAU eyes presented obvious clinical signs of uveitis from 1 to 4 w and reached the peak at 2 w (mean clinical score, 3.8 ± 0.4, n = 6). After administration of the therapeutic formulations, the clinical signs of uveitis, including the engrossed vessels and hypopyon, fade away gradually in all treated groups. There was a statistically significant difference in the mean clinical scores between EAU and other treated groups at week 2 and 4 ($p<0.05$). That was, almost all the therapeutic formulations effectively hindered the development of EAU in Lewis rats immunized with IRBP (Figure 4C). BBR@MSN showed a lower clinical score than BBR at week 1 (mean clinical score, 0.9 ± 0.5 vs. 1.8 ± 0.7, n = 6), which indirectly proved that BBR@MSN prolonged the effective therapeutic time through a sustained release of the targeted drugs. Similarly, DEX@Gel possessed a better efficacy than DEX solution at the terminal observation time (mean clinical score, 0.3 ± 0.5 vs. 0.7 ± 0.5, $p>0.05$, n = 6). More importantly, the eyes treated with BBR@MSN-DEX@Gel had the fewest clinical signs of uveitis and the lowest score during the whole examination term than other groups, especially at week 4 after the treatment, which revealed that BBR@MSN-DEX@Gel exerted better treatment effects than others.

In vivo Drug Release

At week 2 after intravitreal injection of different therapeutic formulations, the results of BBR and DEX concentrations in the IRBP-induced EAU eye tissues (cornea, vitreous body, and retina) are shown in Figure 5. As for the BBR-treated groups (Figure 5A), including BBR, BBR@MSN, and BBR@MSN-DEX@Gel, the concentrations of BBR in both cornea and retina were at a similar level (8.5–25.2 ng/mL) at week 2. However, the BBR concentration in the vitreous body presented an obvious difference, 20.0 ng/mL in BBR, 77.6 ng/mL in BBR@MSN and 76.3 ng/mL in BBR@MSN-DEX@Gel. That was, two kinds of BBR-DDSs sustainably released BBR and provided higher drug concentration than BBR solution. This property fully corroborated that the new formulations might optimize treatment efficacy on EAU, while reducing the administration times. Likewise, DEX@Gel and BBR@MSN-DEX@Gel sustainably released DEX, and provided a higher drug concentration than DEX solution, especially BBR@MSN-DEX@Gel. In addition, according to the previous report,[50] the cytokines secreted by the activated Th 17 cells (eg, interleukin (IL-6)) and monocytes (eg, IL-1β or monocyte chemoattractant protein-1 (MCP-1)) contribute to intraocular inflammation of autoimmune uveitis. Besides, the 50% inhibiting concentration (IC_{50}) values of DEX for the secretion of IL-6, IL-1β and MCP-1 were 3 nM, 7 nM and 3 nM, respectively.[51] Compared to DEX solution and DEX@Gel, only BBR@MSN-DEX@Gel provided enough

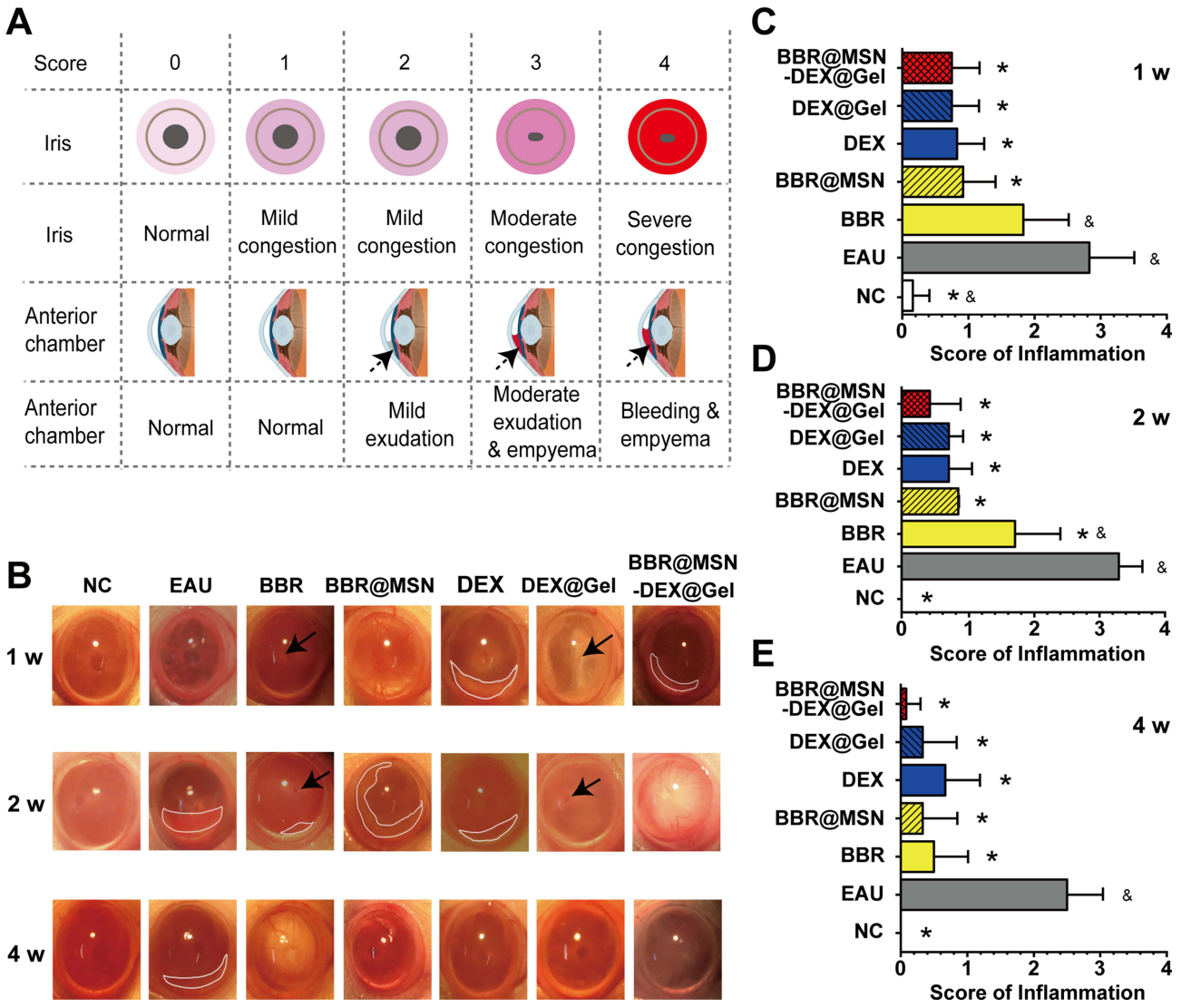

Figure 4 Treatment effectiveness of BBR@MSN-DEX@Gel on IRBP-induced EAU eyes. (**A**) Grading system of uveitis: schematic representation of inflammation manifestation, evaluation indicators, and score sheet. (**B**) Representative photographs of external ocular appearance of NC, EAU, and all treated eyes. (**C**) The mean clinical score of inflammation manifestation of IRBP-induced EAU eyes with or without treatments by BBR solution (BBR), BBR@MSN, DEX solution (DEX), DEX@Gel and BBR@MSN-DEX@Gel (n = 6). *p<0.05 vs EAU and $^{\&}p$<0.05 vs BBR@MSN-DEX@Gel (Two-way ANOVA).

DEX concentrations (> IC_{50} for the secretion of IL-6, IL-1β or MCP-1) in the eye tissues (cornea, vitreous body and retina) within 2 w, which was due to the sustained and long-term DEX release from BBR@MSN-DEX@Gel (Figure 2C and D). Hence, DEX release from BBR@MSN-DEX@Gel was able to maintain the treatment effect on EAU with relatively enough in vivo drug concentration. Based upon the above findings, BBR@MSN-DEX@Gel presented some synergistic anti-inflammation efficacy on EAU treatment (2 w).

Histopathological Examination

Histopathological evaluations of all treated eyes were performed at the set time points (Figure 6). In the NC group, complete and smooth histopathological structures of retina and iris were observed at week 1, 2 and 4. After EAU was induced by IRBP subcutaneous injection, cellular immune reactions were stimulated, which could be further categorized into two stages: active (1–2 w) and inactive (2–4 w).[52] In the active stage of EAU eyes, the classic manifestations were observed, such as inflammatory infiltration or exudation (#), disorganization or detachment (Δ) (2 w-retina-Masson-EAU in Figure 6A), and retinal fold (arrow, 1 w-retina-H&E-EAU in Figure 6A), as previously reported.[53,54] Then the immune

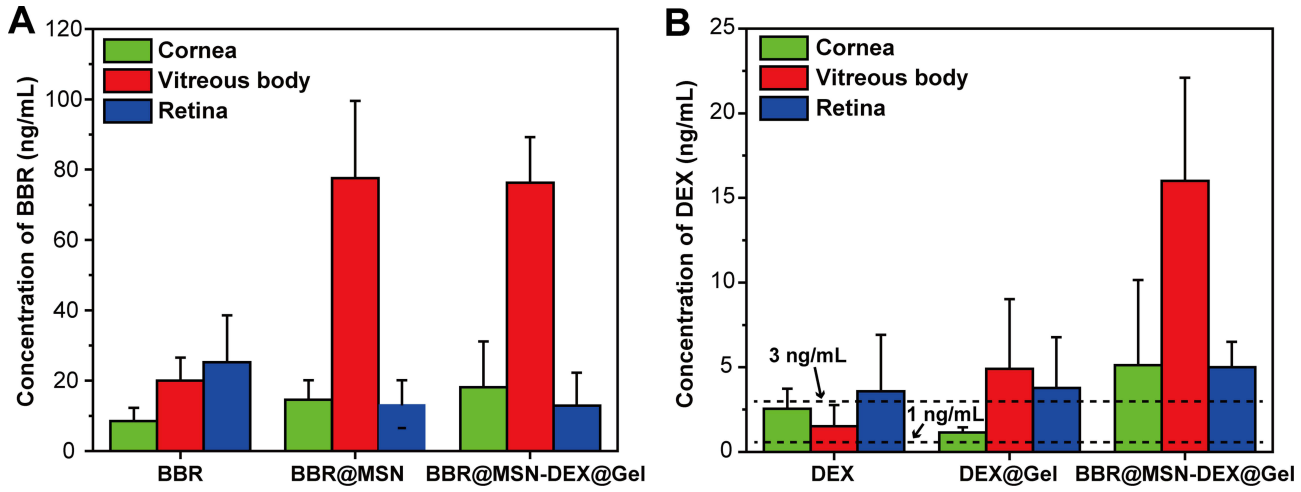

Figure 5 In vivo drug release of (**A**) BBR from BBR@MSN and BBR@MSN-DEX@Gel, and (**B**) DEX from DEX@Gel and BBR@MSN-DEX@Gel in eye tissues (cornea, vitreous body, and retina) at week 2 after single intravitreal injection of different therapeutic formulations (n = 4).

reactions in the EAU eyes entered the inactive stage (2–4 w), in which inflammatory infiltration or exudation gradually faded (Figure 6A). As far as the treated groups, the obvious inflammatory manifestations appeared at week 1, including inflammatory infiltration or exudation, and retinal fold (such as 1 w-retina-H&E-BBR@MSN-DEX@Gel in Figure 6A). And then the above-mentioned inflammatory reactions gradually faded from 2 to 4 w. The active stage in the treated groups was shortened, while the inactive stage was in advance. The two stages of immune reactions shown in the EAU eyes (active, 1–2 w; inactive, 2–4 w) were corrected in the treated groups, which might be attributed to the treatment effects of therapeutic formulations (BBR@MSN, DEX@Gel and BBR@MSN-DEX@Gel). Compared with the EAU group, BBR@MSN, DEX@Gel and BBR@MSN-DEX@Gel obviously reduced inflammatory reactions, especially in the later part of the active stage (week 2). In addition, BBR@MSN-DEX@Gel showed the optimal treatment efficacy, which mainly resulted from the synergistic anti-inflammation efficacy during the whole treatment. As far as the obvious ocular inflammatory reactions at week 1 in the treated groups, they were mainly due to the ocular trauma by intravitreal injection of different therapeutic formulations. It was noted that IRBP-induced EAU was carried out by a subcutaneous injection, which could not cause any ocular trauma or possible immune responses.

Based on the taken images, we further analyzed the inflammatory reactions (n = 12 images), and the statistical results are shown in Figure 6B. The EAU eyes had higher histopathological scores than the NC ($p<0.05$) at all time points, which verified the successful establishment of EAU models with characteristic manifestations of posterior uveitis.[55] The pathological score of EAU model reached its peak at week 2 (3.9 ± 0.2) and then decreased to 2.2 ± 0.9 at week 4, which was well supported by the histopathological and clinical observations (Figure 6A). After intravitreal administration of therapeutic formulations, the treated eyes presented higher inflammatory scores in BBR@MSN (2.4 ± 0.6), DEX@Gel (3.5 ± 0.5) or BBR@MSN-DEX@Gel (3.3 ± 0.3) than EAU group (2.0 ± 0.7) at week 1, which mainly resulted from the more ocular trauma in the treated groups than IRBP-induced EAU. Then, the inflammatory score dramatically declined in BBR@MSN (1.4 ± 0.6), DEX@Gel (1.5 ± 0.5) and BBR@MSN-DEX@Gel (0.6 ± 0.5) at week 2, compared with that in EAU group which reached its peak (3.9 ± 0.2) at the same time point. Interestingly, compared to DEX@Gel and BBR@MSN, BBR@MSN-DEX@Gel maintained a lower level ($p<0.05$) at week 2. This was supported by the more in vitro DEX release from BBR@MSN-DEX@Gel (~65.2%, Figure 2D) and in vivo DEX concentration in the detected vitreous body (16.5 ng/mL, Figure 5B) than DEX@Gel (~39.5%, 11.7 ng/mL) at week 2. Moreover, the addition of BBR@MSN into DEX@Gel to form BBR@MSN-DEX@Gel also improved the therapeutic effect on EAU. Thereafter, our findings fully revealed that this dual-drug nanocomposite formulation may be a valuable therapeutic agent for the suppression of autoimmune uveitis.

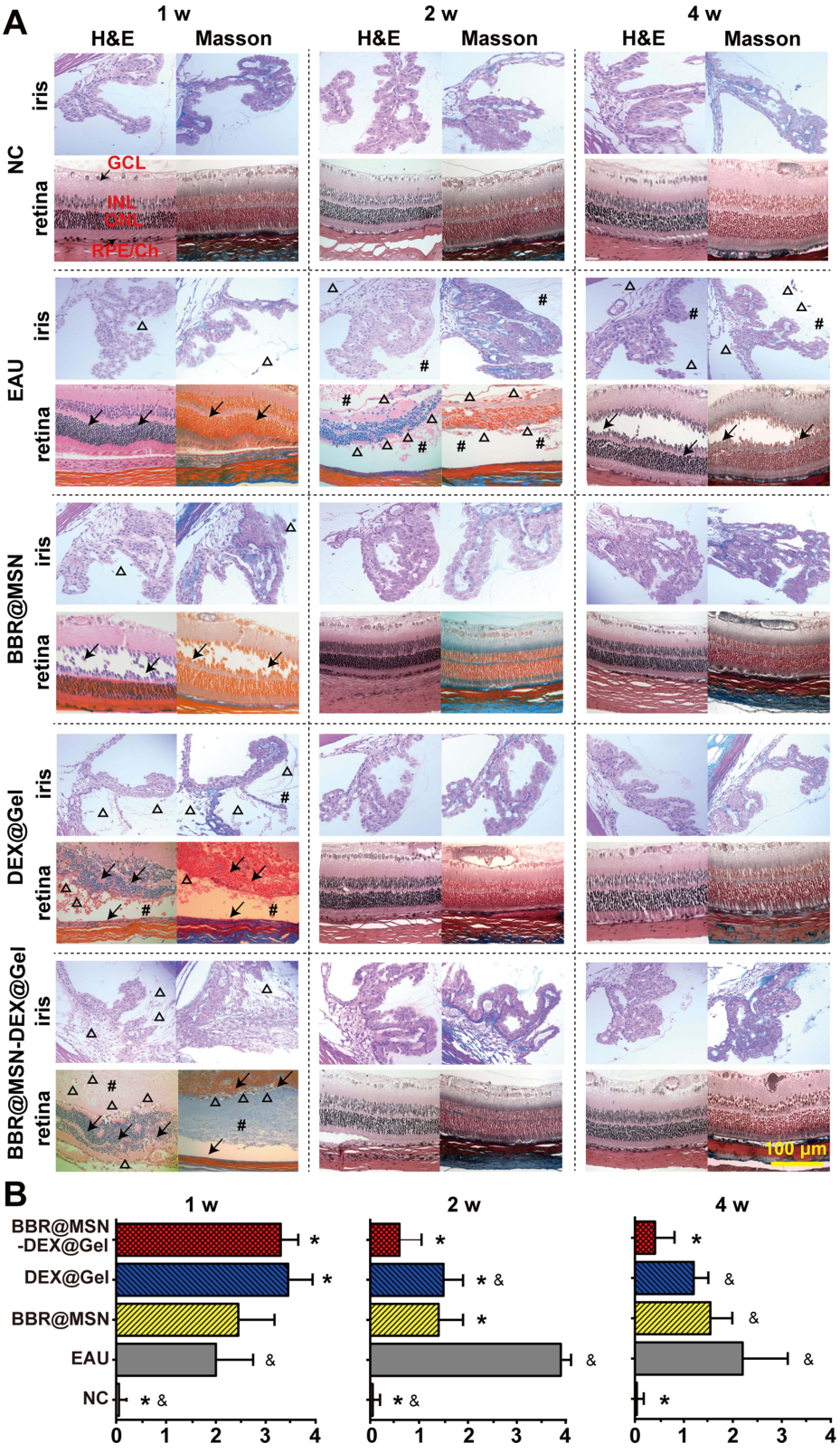

Figure 6 Histopathological examination. (**A**) Representative images of eye tissues, and (**B**) inflammatory evaluation scores in NC, EAU, and the treated groups (BBR@MSN, DEX@Gel and BBR@MSN-DEX@Gel, n = 3). At week 1, 2 and 4 after EAU and administration of the therapeutic formulations, all eyes were fixed and the tissue sections of retina and iris were stained by H&E and Masson. Several noteworthy histological reactions were pointed out with specific indicators, including # (inflammatory exudation), Δ (disorganization or detachment), arrow (retinal fold). *p<0.05 vs EAU and $^{\&}p$<0.05 vs BBR@MSN-DEX@Gel (Two-way ANOVA).

Discussion

As is well known, glucocorticoids (eg, DEX) remain the mainstay therapy for autoimmune uveitis with powerful anti-inflammatory activities, even though their anti-inflammatory effects are complex and incompletely understood.[4] The primary anti-inflammatory actions appear to be mediated by the inhibition of pro-inflammatory transcription factors and the suppression of prostaglandin and interleukin synthesis.[56,57] However, long-term administrations of DEX may cause serious and undesirable ocular or systemic side effects, such as elevated IOP, cataract formation and osteoporosis.[5] Thus, combined therapy targeting different pathophysiological mechanisms should be explored to treat autoimmune uveitis. BBR shows anti-inflammatory activities along with a good safety profile.[58] BBR can affect chronic inflammation (eg, autoimmune uveitis) by suppression of Th17 cell cytokines (IL-17A).[59,60] So, BBR and DEX were chosen as the therapeutic agents for the EAU treatment because of their anti-inflammatory bioactivities. In order to simultaneously encapsulate and effectively deliver two kinds of small molecule drugs, we developed a novel dual-drug nanocomposite formulation based on MSNs/thermogel composite materials which presented excellent biocompatibility and biodegradability, high drug-loading efficiency,[36] perfect drug bioavailability[42,61] and sustainably release property.[37,39]

In all drug-loading processes, the stirring-drying course was used to load BBR into the surface-modified MSNs to form BBR@MSN, which was then encapsulated into the thermogel precursor solution to prepare BBR@MSN-DEX@Gel. No centrifuge separation and washing processes were involved, and there was no drug loss during the whole preparation process. Thus, the encapsulation efficiencies of BBR and DEX into MSNs and thermogel were all thought as ~100%.[41] And the drug loading of BBR and DEX in the BBR@MSN, DEX@Gel and BBR@MSN-DEX@Gel could be calculated according to the feeding amounts of BBR, DEX and MSNs in the thermogel precursor solution. That was, BBR@MSN-DEX@Gel thermogel precursor solution (1 μL) contains 2.0 μg DEX, 3.3 μg BBR, 6.7 μg MSNs and 0.25 mg copolymer. Specifically, the drug loading amount of BBR was 33% in the BBR@MSN and 0.33% in the BBR@MSN-DEX@Gel, while the drug loading amount of DEX was 0.20% in both DEX@Gel and BBR@MSN-DEX@Gel. In all experiments, the same amount of BBR was used in the BBR@MSN and BBR@MSN-DEX@Gel groups, also the amount of DEX in the DEX@Gel and BBR@MSN-DEX@Gel groups.

The above loading amounts of BBR and DEX in the BBR@MSN, DEX@Gel and BBR@MSN-DEX@Gel presented high biological safety and suitable for in vivo applications. It has been reported that a single subconjunctival injection of dexamethasone pro-drug microcrystals (containing 5 μg/μL DEX) in EAU rat eyes did not cause obvious retinal toxic reaction and elevated IOP.[23] This dosage was 2.5 times higher than that used in this study (2.0 μg/μL DEX), which demonstrated the in vivo biosafety of BBR@MSN-DEX@Gel. For the other, the reported C_{max} of BBR in the aqueous humor after an administration of BBR compound liposomes was 400.02 ng/mL,[30] which was more than 5 times than that in this study (76.3 ng/mL BBR in the eye vitreous body after single intravitreal injection of BBR@MSN-DEX@Gel). As a consequence, the chosen concentrations of DEX and BBR were safe enough for the intraocular administration. In this study, both BBR@MSN and BBR@MSN-DEX@Gel exhibited the initial burst releases with the immediate BBR concentrations of 15.9 and 16.2 μg/mL on day 1 (Figure 2A), respectively. BBR@MSN-DEX@Gel only showed a slight BBR "burst release" (about 23% cumulative release within 8h, Figure 2B), which was superior to that in the previous report (~40%, 8h).[48] Moreover, both DEX@Gel and BBR@MSN-DEX@Gel provided the immediate DEX concentrations of 13.9 μg/mL and 24.7 μg/mL (Figure 2C), responding to the cumulative releases of 11.7% and 18.9%, respectively (Figure 2D). The rapid initial releases of DEX and BBR from BBR@MSN-DEX@Gel could inhibit inflammation at the early stage which was beneficial to the treatment of EAU without obvious drug toxicity.[23]

Recently, both BBR[59] and DEX[57,62] have been gradually employed owing to their ability to continuously reduce the inflammation reactions and secretion of pro-inflammatory cytokines. The results shown in this study fully illustrated the more effective treatment of BBR@MSN-DEX@Gel in alleviating ocular inflammation in EAU treatment than single-component formulations. However, the obtained data in this study only provided some preliminary evidence that BBR@MSN-DEX@Gel could treat EAU. Exploring the pharmacokinetics and anti-inflammatory mechanisms of BBR@MSN-DEX@Gel for EAU treatment should be pursued as soon as possible.

Conclusion

In this study, we successfully developed a novel dual-drug nanocomposite formulation by integrating berberine (BBR)-loaded mesoporous silica nanoparticles (MSNs) into dexamethasone (DEX)-loaded thermogel (BBR@MSN-DEX@Gel), and further assessed the combined therapy effectiveness of the BBR@MSN-DEX@Gel on autoimmune experimental uveitis. The prepared BBR@MSN-DEX@Gel possessed a sustained in vitro drug release till 6 weeks, with minimal in vitro cytotoxicity. Compared with the single-component drug (BBR or DEX), the BBR@MSN-DEX@Gel formulation exhibited an overwhelming therapeutic advantage on IRBP-induced autoimmune experimental uveitis for up to 28 days without inducing any obvious histological pathology changes. Thus, this novel dual-drug nanocomposite formulation was expected to acquire an overwhelming treatment effect with a less dose and longer treatment duration and possessed great potential for future autoimmune uveitis therapy.

Abbreviations

DEX, dexamethasone acetate; BBR, berberine hydrochloride; DDSs, drug delivery systems; DLS, dynamic light scattering; LPS, lipopolysaccharide; HConEpics, human conjunctival epithelial cells; IL-17A, interleukin-17A; MCP-1, monocyte chemoattractant protein-1; MSNs, mesoporous silica nanoparticles; thermogel, thermosensitive nanogel; PLGA–PEG–PLGA, poly-(lactic acid co-glycolic acid)–polyethylene glycol–poly-(lactic acid co-glycolic acid); CFA, complete freund's adjuvant; EAU, experimental autoimmune uveitis; calcein-AM, calcein acetoxymethyl ester; PI, propidium iodide; FBS, fetal bovine serum; PBS, phosphate-buffered saline; TA, tartaric acid; EDC, 1-(3-dimethylaminopropyl)-3-ethylcarbodiimide hydrochloride; NHS, N-hydroxysuccinimide; IC_{50}, 50% inhibiting concentration; H&E, hematoxylin & eosin.

Acknowledgments

The authors acknowledge the support from the National Natural Science Foundation of China (82274060), the Scientific and Innovative Action Plan of Shanghai (19441900600), and the Natural Science Foundation of Shanghai (19ZR1408300), the Science and Technology Commission of Shanghai Municipality (21Y11909900) and Shanghai Municipal Health Commission (202240316). The sponsor or funding organization had no role in the design or conduct of this research.

Disclosure

The authors report no conflicts of interest in this work.

References

1. Tsirouki T, Dastiridou A, Symeonidis C, et al. A focus on the epidemiology of uveitis. *Ocul Immunol Inflamm*. 2018;26(1):2–16. doi:10.1080/09273948.2016.1196713
2. Selmi C. Diagnosis and classification of autoimmune uveitis. *Autoimmun Rev*. 2014;13(4–5):591–594. doi:10.1016/j.autrev.2014.01.006
3. Joltikov KA, Lobo-Chan AM. Epidemiology and risk factors in non-infectious uveitis: a systematic review. *Front Med Prc*. 2021;8:695904. doi:10.3389/fmed.2021.695904
4. Li H, Zhang Z, Li Y, et al. Therapeutic effect of rapamycin-loaded small extracellular vesicles derived from mesenchymal stem cells on experimental autoimmune uveitis. *Front Immunol*. 2022;13:864956. doi:10.3389/fimmu.2022.864956
5. Fassbender Adeniran JM, Jusufbegovic D, Schaal S. Common and rare ocular side-effects of the dexamethasone implant. *Ocul Immunol Inflamm*. 2017;25(6):834–840. doi:10.1080/09273948.2016.1184284
6. Ehteshamfar SM, Akhbari M, Afshari JT, et al. Anti-inflammatory and immune-modulatory impacts of berberine on activation of autoreactive T cells in autoimmune inflammation. *J Cell Mol Med*. 2020;24(23):3573–3588. doi:10.1111/jcmm.16049
7. Jin J, Xu M, Liu Y, et al. Alginate-based composite microspheres coated by berberine simultaneously improve hemostatic and antibacterial efficacy. *Colloids Surf B*. 2020;194:111168. doi:10.1016/j.colsurfb.2020.111168
8. Lin J, Cai Q, Liang B, et al. Berberine, a traditional Chinese medicine, reduces inflammation in adipose tissue, polarizes M2 macrophages, and increases energy expenditure in mice fed a high-fat diet. *Med Sci Monit*. 2019;25:87–97. doi:10.12659/MSM.911849
9. Gote V, Sikder S, Sicotte J, Pal D. Ocular drug delivery: present innovations and future challenges. *J Pharmacol Exp Ther*. 2019;370(3):602–624. doi:10.1124/jpet.119.256933
10. Dosmar E, Walsh J, Doyel M, et al. Targeting ocular drug delivery: an examination of local anatomy and current approaches. *Bioengineering*. 2022;9(1):41. doi:10.3390/bioengineering9010041
11. Machinaga N, Ashley GW, Reid R, et al. A controlled release system for long-acting intravitreal delivery of small molecules. *Transl Vis Sci Technol*. 2018;7(4):21. doi:10.1167/tvst.7.4.21

12. Del Amo EM, Urtti A. Rabbit as an animal model for intravitreal pharmacokinetics: clinical predictability and quality of the published data. *Exp Eye Res*. 2015;137:111–124. doi:10.1016/j.exer.2015.05.003
13. Zhang J, Jiao J, Niu M, et al. Ten years of knowledge of nano-carrier based drug delivery systems in ophthalmology: current evidence, challenges, and future prospective. *Int J Nanomed*. 2021;16:6497–6530. doi:10.2147/IJN.S329831
14. Ridha AA, Kashanian S, Azandaryani AH, Rafipour R, Mahdavian E. New folate-modified human serum albumin conjugated to cationic lipid carriers for dual targeting of mitoxantrone against breast cancer. *Curr Pharm Biotechno*. 2020;21(4):305–315. doi:10.2174/1389201020666191114113022
15. Rezaei S, Kashanian S, Bahrami Y, Cruz LJ, Motiei M. Redox-sensitive and hyaluronic acid-functionalized nanoparticles for improving breast cancer treatment by cytoplasmic 17alpha-methyltestosterone delivery. *Molecules*. 2020;25(5):1181. doi:10.3390/molecules25051181
16. Gomhor JAH, Kashanian S, Rafipour R, Mahdavian E, Mansouri K. Development and characterization of folic acid-functionalized apoferritin as a delivery vehicle for epirubicin against MCF-7 breast cancer cells. *Artif Cells Nanomed Biotechnol*. 2018;46(3):847–854. doi:10.1080/21691401.2018.1516671
17. Hemati Azandaryani A, Kashanian S, Derakhshandeh K. Folate conjugated hybrid nanocarrier for targeted letrozole delivery in breast cancer treatment. *Pharmaceut Res*. 2017;34(12):2798–2808. doi:10.1007/s11095-017-2260-x
18. Bao Z, Yu A, Shi H, et al. Glycol chitosan/oxidized hyaluronic acid hydrogel film for topical ocular delivery of dexamethasone and levofloxacin. *Int J Biol Macromol*. 2021;167:659–666. doi:10.1016/j.ijbiomac.2020.11.214
19. Balla A, Ruponen M, Valtari A, et al. Understanding dexamethasone kinetics in the rabbit tear fluid: drug release and clearance from solution, suspension and hydrogel formulations. *Eur J Pharm Biopharm*. 2022;172:53–60. doi:10.1016/j.ejpb.2022.01.005
20. Di Prima G, Licciardi M, Bongiovi F, Pitarresi G, Giammona G. Inulin-based polymeric micelles functionalized with ocular permeation enhancers: improvement of dexamethasone permeation/penetration through bovine corneas. *Pharmaceutics*. 2021;13(9):1431. doi:10.3390/pharmaceutics13091431
21. Yavuz B, Pehlivan SB, Vural I, Unlu N. In vitro/in vivo evaluation of dexamethasone-PAMAM dendrimer complexes for retinal drug delivery. *J Pharm Sci*. 2015;104(11):3814–3823. doi:10.1002/jps.24588
22. Gan L, Han S, Shen J, et al. Self-assembled liquid crystalline nanoparticles as a novel ophthalmic delivery system for dexamethasone: improving preocular retention and ocular bioavailability. *Int J Pharm*. 2010;396(1–2):179–187. doi:10.1016/j.ijpharm.2010.06.015
23. Cai M, Xu Z, Zhou X, et al. Long-acting acid-sensitive ketal-linked dexamethasone microcrystals for treating experimental autoimmune uveitis. *APL Bioeng*. 2022;6(4):046101. doi:10.1063/5.0118311
24. González-Fernández FM, Delledonne A, Nicoli S, et al. Nanostructured lipid carriers for enhanced transscleral delivery of dexamethasone acetate: development, ex vivo characterization and multiphoton microscopy studies. *Pharmaceutics*. 2023;15(2):407. doi:10.3390/pharmaceutics15020407
25. Kumari S, Dandamudi M, Rani S, et al. Dexamethasone-loaded nanostructured lipid carriers for the treatment of dry eye disease. *Pharmaceutics*. 2021;13(6):905. doi:10.3390/pharmaceutics13060905
26. Karti O, Saatci AO. Place of intravitreal dexamethasone implant in the treatment armamentarium of diabetic macular edema. *World J Diabetes*. 2021;12(8):1220–1232. doi:10.4239/wjd.v12.i8.1220
27. Boyer DS, Yoon YH, Belfort R, et al. Three-year, randomized, sham-controlled trial of dexamethasone intravitreal implant in patients with diabetic macular edema. *Ophthalmology*. 2014;121(10):1904–1914. doi:10.1016/j.ophtha.2014.04.024
28. Sella R, Oray M, Friling R, Umar L, Tugal-Tutkun I, Kramer M. Dexamethasone intravitreal implant (Ozurdex®) for pediatric uveitis. *Graefes Arch Clin Exp Ophthalmol*. 2015;253(10):1777–1782. doi:10.1007/s00417-015-3124-x
29. Jawed Khan M, Hafeez A, Aftab Siddiqui M. Nanocarrier based delivery of berberine: a critical review on pharmaceutical and preclinical characteristics of the bioactive. *Curr Pharm Biotechno*. 2023;24(11):1449–1464. doi:10.2174/1389201024666230112141330
30. Lai S, Wei Y, Wu Q, et al. Liposomes for effective drug delivery to the ocular posterior chamber. *J Nanobiotechnol*. 2019;17(1):64. doi:10.1186/s12951-019-0498-7
31. Liu R, Liu Z, Zhang C, Zhang B. Gelucire44/14 as a novel absorption enhancer for drugs with different hydrophilicities: in vitro and in vivo improvement on transcorneal permeation. *J Pharm Sci*. 2011;100(8):3186–3195. doi:10.1002/jps.22540
32. Carucci C, Scalas N, Porcheddu A, Piludu M, Monduzzi M, Salis A. Adsorption and release of sulfamethizole from mesoporous silica nanoparticles functionalised with triethylenetetramine. *Int J Mol Sci*. 2021;22(14):7665. doi:10.3390/ijms22147665
33. Choi JK, Park JY, Lee S, et al. Greater plasma protein adsorption on mesoporous silica nanoparticles aggravates atopic dermatitis. *Int J Nanomed*. 2022;17:4599–4617. doi:10.2147/IJN.S383324
34. Sun J, Nie H, Pan P, et al. Combined anti-angiogenic and anti-inflammatory nanoformulation for effective treatment of ocular vascular diseases. *Int J Nanomed*. 2023;18:437–453. doi:10.2147/IJN.S387428
35. Hu C, Sun J, Zhang Y, et al. Local delivery and sustained-release of nitric oxide donor loaded in mesoporous silica particles for efficient treatment of primary open-angle glaucoma. *Adv Healthc Mater*. 2018;7(23):e1801047. doi:10.1002/adhm.201801047
36. Croissant JG, Fatieiev Y, Almalik A, Khashab NM. Mesoporous silica and organosilica nanoparticles: physical chemistry, biosafety, delivery strategies, and biomedical applications. *Adv Healthc Mater*. 2018;7(4):1700831.
37. Yue Q, Zhang Y, Jiang Y, et al. Nanoengineering of core-shell magnetic mesoporous microspheres with tunable surface roughness. *J Am Chem Soc*. 2017;139(13):4954–4961. doi:10.1021/jacs.7b01464
38. Liu X, Fan H, Meng Z, et al. Combined silver sulfadiazine nanosuspension with thermosensitive hydrogel: an effective antibacterial treatment for wound healing in an animal model. *Int J Nanomed*. 2023;18:679–691. doi:10.2147/IJN.S395004
39. Lyu N, Zhao Y, Xiang J, et al. Inhibiting corneal neovascularization by sustainably releasing anti-VEGF and anti-inflammation drugs from silica-thermogel nanohybrids. *Mat Sci Eng C Mater*. 2021;128:112274. doi:10.1016/j.msec.2021.112274
40. Sun J, Lei Y, Dai Z, et al. Sustained release of brimonidine from a new composite drug delivery system for treatment of glaucoma. *ACS Appl Mater Interfaces*. 2017;9(9):7990–7999. doi:10.1021/acsami.6b16509
41. Sun J, Liu X, Lei Y, et al. Sustained subconjunctival delivery of cyclosporine A using thermogelling polymers for glaucoma filtration surgery. *J Mater Chem B*. 2017;5(31):6400–6411. doi:10.1039/C7TB01556A
42. Zhang S, Fang Y, Sun J, Deng Y, Lu Y. Improved treatment on ocular inflammation with rationally designed thermoresponsive nanocomposite formulation. *Adv Ther*. 2021;4(10):2100088. doi:10.1002/adtp.202100088

43. Lan H, An P, Liu Q, et al. Aidi injection induces apoptosis of hepatocellular carcinoma cells through the mitochondrial pathway. *J Ethnopharmacol*. 2021;274:114073. doi:10.1016/j.jep.2021.114073
44. Zhao Y, Huang C, Zhang Z, et al. Sustained release of brimonidine from BRI@SR@TPU implant for treatment of glaucoma. *Drug Deliv*. 2022;29 (1):613–623. doi:10.1080/10717544.2022.2039806
45. Copland DA, Wertheim MS, Armitage WJ, Nicholson LB, Raveney BJ, Dick AD. The clinical time-course of experimental autoimmune uveoretinitis using topical endoscopic fundal imaging with histologic and cellular infiltrate correlation. *Invest Ophth Vis Sci*. 2008;49 (12):5458–5465. doi:10.1167/iovs.08-2348
46. Kohno H, Sakai T, Saito S, Okano K, Kitahara K. Treatment of experimental autoimmune uveoretinitis with atorvastatin and lovastatin. *Exp Eye Res*. 2007;84(3):569–576. doi:10.1016/j.exer.2006.11.011
47. Caspi RR, Roberge FG, McAllister CG, et al. T cell lines mediating experimental autoimmune uveoretinitis (EAU) in the rat. *J Immunol*. 1986;136 (3):928–933. doi:10.4049/jimmunol.136.3.928
48. Bhatnagar P, Kumari M, Pahuja R, et al. Hyaluronic acid-grafted PLGA nanoparticles for the sustained delivery of berberine chloride for an efficient suppression of Ehrlich ascites tumors. *Drug Deliv Transl Re*. 2018;8(3):565–579. doi:10.1007/s13346-018-0485-9
49. Zhong Z, Su G, Kijlstra A, Yang P. Activation of the interleukin-23/interleukin-17 signalling pathway in autoinflammatory and autoimmune uveitis. *Prog Retin Eye Res*. 2021;80:100866. doi:10.1016/j.preteyeres.2020.100866
50. Weinstein JE, Pepple KL. Cytokines in uveitis. *Curr Opin Ophthalmol*. 2018;29(3):267–274. doi:10.1097/ICU.0000000000000466
51. Nehme A, Edelman J. Dexamethasone inhibits high glucose–, TNF-α–, and IL-1β–induced secretion of inflammatory and angiogenic mediators from retinal microvascular pericytes. *Invest Ophth Vis Sci*. 2008;49(5):2030–2038. doi:10.1167/iovs.07-0273
52. Yang P. Editorial: uveitis: pathology, molecular mechanisms and therapy. *Curr Mol Med*. 2018;17(7):459. doi:10.2174/1566524018666180207161909
53. Fang CB, Zhou DX, Zhan SX, et al. Amelioration of experimental autoimmune uveitis by leflunomide in Lewis rats. *PLoS One*. 2013;8(4):e62071. doi:10.1371/journal.pone.0062071
54. Luo L, Yang J, Oh Y, et al. Controlled release of corticosteroid with biodegradable nanoparticles for treating experimental autoimmune uveitis. *J Controlled Release*. 2019;296:68–80. doi:10.1016/j.jconrel.2019.01.018
55. Singh RB, Sinha S, Saini C, Elbasiony E, Thakur S, Agarwal A. Recent advances in the management of non-infectious posterior uveitis. *Int Ophthalmol*. 2020;40(11):3187–3207. doi:10.1007/s10792-020-01496-0
56. Panettieri RA, Schaafsma D, Amrani Y, Koziol-White C, Ostrom R, Tliba O. Non-genomic effects of glucocorticoids: an updated view. *Trends Pharmacol Sci*. 2019;40(1):38–49. doi:10.1016/j.tips.2018.11.002
57. Stimpson ML, Lait PJP, Schewitz-Bowers LP, et al. IL-10 and IL-17 expression by CD4(+) T cells is altered in corticosteroid refractory immune thrombocytopenia (ITP). *J Thromb Haemost*. 2020;18(10):2712–2720. doi:10.1111/jth.14970
58. Tillhon M, Guaman Ortiz LM, Lombardi P, Scovassi AI. Berberine: new perspectives for old remedies. *Biochem Pharmacol*. 2012;84 (10):1260–1267. doi:10.1016/j.bcp.2012.07.018
59. Li YH, Xiao HT, Hu DD, et al. Berberine ameliorates chronic relapsing dextran sulfate sodium-induced colitis in C57BL/6 mice by suppressing Th17 responses. *Pharmacol Res*. 2016;110:227–239. doi:10.1016/j.phrs.2016.02.010
60. Jia X, Jia L, Mo L, et al. Berberine ameliorates periodontal bone loss by regulating gut microbiota. *J Dent Res*. 2019;98(1):107–116. doi:10.1177/0022034518797275
61. Song H, Ahmad Nor Y, Yu M, et al. Silica nanopollens enhance adhesion for long-term bacterial inhibition. *J Am Chem Soc*. 2016;138 (20):6455–6462. doi:10.1021/jacs.6b00243
62. Yang K, Wen J, Liu X, et al. Inhibitory effect of rapamycin and dexamethasone on production of IL-17 and IFN-gamma in Vogt-Koyanagi-Harada patients. *Brit J Ophthalmol*. 2009;93(2):249–253. doi:10.1136/bjo.2008.142489